Numerical Test of the Onsager Relations in a Driven System

Xipeng Wang[*]

Key Laboratory of Soft Matter Physics, Institute of Physics, Chinese Academy of Sciences, Beijing 100190, China

Jure Dobnikar[†]

Key Laboratory of Soft Matter Physics, Institute of Physics, Chinese Academy of Sciences, Beijing 100190, China
School of Physical Sciences, University of Chinese Academy of Sciences, Beijing 100049, China,
and Songshan Lake Materials Laboratory, Dongguan, Guangdong 523808, China

Daan Frenkel[‡]

Yusuf Hamied Department of Chemistry, University of Cambridge Lensfield Road, Cambridge CB2 1EW, United Kingdom

The Onsager reciprocity relations were formulated in the context of irreversible thermodynamics, but they are based on assumptions that have a wider applicability. Here, we present simulations testing the Onsager relations between surface-coupled diffusive and bulk fluxes in a system prepared in a nonequilibrium steady state. The system consists of a mixture of two identical species maintained at different temperatures inside a channel. In order to tune the friction of the two species with the walls independently, while keeping the particle-wall interaction potentials the same, we allow the kinematics of particle-wall collisions to be different: "bounce-back" (*B*) or "specular" (*S*). In the *BB* case, diffusio-capillary transport can only take place if the two species have different temperatures. We find that the Onsager reciprocity relations are obeyed in the linear regime, even in the *BB* case where all fluxes are the result of perturbing the system from a nonequilibrium steady state in a way that does not satisfy time-reversal symmetry. Our Letter provides a direct, numerical illustration of the validity of the Onsager relations outside their original range of application, and suggests their relevance for transport in driven or active systems.

Introduction.—The theory of irreversible thermodynamics deals with the situation where there is a linear relation between thermodynamic fluxes $\mathbf{j}_\alpha$ and the thermodynamic driving forces $\mathbf{X}_\beta$: here, α denotes the type of flux (heat flux, diffusion flux, volume flow, etc.) and β denotes the different forces: $\nabla 1/T$, $\nabla \mu/T$, $\nabla P/T$, etc. In general, forces are not just driving their "conjugate" flux, such as when $\nabla 1/T$ is driving the heat flux, but also other fluxes, as long as the coupling is symmetry allowed. The constitutive equations are then of the form

$$\mathbf{j}_\alpha = \mathcal{L}_{\alpha\beta} \mathbf{X}_\beta. \qquad (1)$$

Onsager [1] showed that, for nonrotating systems, and in the absence of magnetic fields, the transport matrix $\mathcal{L}$ is symmetric. There exist many derivations of the Onsager reciprocity theorem, but the simplest, and most general one (see, e.g., [2]) shows that only a few properties of the state variables of the system are important: (1) the probability distribution of fluctuations must be locally Gaussian, (2) the driving forces are the spatial derivatives of the log of the probability distribution of the state variables, (3) the relation between fluxes and small driving forces is linear, and (4) the underlying equations of motion

satisfy microscopic reversibility. The above conditions do not restrict the reciprocal relations to systems weakly perturbed from the thermodynamic equilibrium. However, their validity is not self-evident for systems [3] that are driven to a strongly nonequilibrium steady state.

In this Letter, we test the validity of the Onsager reciprocal relations for a simple model of a driven nonequilibrium system where fluxes and driving forces are well defined. Our model is chosen such that it is in a nonequilibrium steady state, even in the absence of driving forces. Importantly, the underlying equations of motion of the driven system do not satisfy microscopic reversibility. We first verify that the Onsager relations hold in the limit where we apply forces to the system that fluctuates around equilibrium, and subsequently test if they remain valid when the system is initially in a steady state far from the thermodynamic equilibrium. We note that the Onsager relations have been extensively verified in experiments on systems perturbed from equilibrium (for an early review, see Ref. [4]), but to a lesser extent in simulations (see e.g., Ref. [5]). In particular, there are, to our knowledge, no systematic numerical tests of the Onsager relations for systems that are perturbed from a nonequilibrium steady state. One reason may be that is not easy to achieve
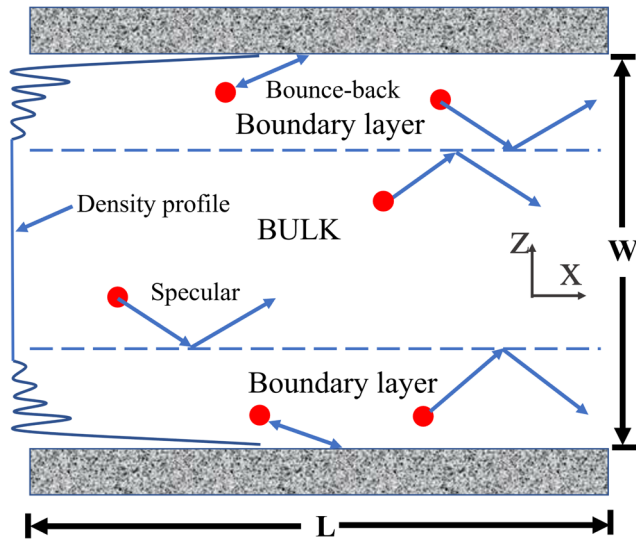
FIG. 1. Schematic illustration of the system: the fluid of hot and cold particles is confined between two parallel flat square walls with size $L \times L$ fixed at a separation W in the z direction. The system is periodically extended in the x and y directions and all the forces are applied in the x direction. The drawing represents an xz cross section of the system. It illustrates the specular and bounce-back collision rules. Dashed lines represent infinitely thin specular walls implemented to determine the fluxes in the "bulk" of the channel (see text). Particles on either side of such a wall can interact with each other. However, they cannot cross these walls: rather they undergo specular reflection.

sufficient numerical accuracy, because surface-induced coupling of fluxes is usually weak, and long runs are needed to perform meaningful tests of the Onsager relations.

In our simulations, we consider an equimolar fluid mixture of two components [labeled hot (H) and cold (C)] in a channel bounded by two flat hard walls at a distance $\Delta z = W$. Periodic boundary conditions are applied in x and y directions. Figure 1 shows the schematic setup of the simulations.

The proper description of the relation between forces and fluxes requires some care, as we cannot assume that the local-equilibrium relations of irreversible thermodynamics hold.

For systems perturbed from equilibrium at a fixed temperature T, the fluxes of the particles are driven by the gradients of the chemical potentials of the two species, or equivalently, by a pressure gradient and a chemical potential gradient at constant pressure: in the absence of cross couplings, the pressure gradient causes a bulk flow, but no diffusive flux and the chemical potential gradient causes a diffusive flux, but no bulk flow.

In simulations of systems with periodic boundaries, it is often convenient to replace $-\nabla\mu_i$, the gradient of the chemical potential of species i by an equivalent "color" force F_i, which acts only on that species [6–8]. In what follows, we will study the response to imposed color forces

of a driven system. The reason why we consider the effect of color forces, rather than that of $-\nabla\mu_i$, is that mechanical forces keep their meaning even for systems far from thermodynamic equilibrium [see Supplemental Material (SM) [9]].

All particles interact through the same, purely repulsive Weeks-Chandler-Andersen potential [10]: $u(r) = 4\epsilon[(\sigma/r)^{12} - (\sigma/r)^6 + 1/4]$ for $r < 2^{1/6}\sigma$, and $u(r) = 0$ elsewhere. In what follows, we will use reduced units, such that the units of length, energy, and mass are, respectively, σ, ϵ, and m (the mass of a particle). The unit of time is then $\sqrt{m\sigma^2/\epsilon}$.

In our Letter, we maintain two classes of particles at different temperatures: hot and cold. The H and C particles are subject to "color forces" F_H and F_C acting along the x direction. We consider an equimolar mixture of H and C particles. The total number of particles, $N \equiv N_C + N_H$, was either 1000 or 2000 (see below). We carried out simulations at a number density $\rho = N/(L^2 W) = 0.405$. In general, in the simulations of driven systems, the boundaries have an effect on the behavior. In order to be able to separate bulk from boundary-induced properties, we worked with sufficiently wide channels, i.e., the width W is chosen such that a slab in the middle of the channel (the "bulk") is not affected by the boundaries: $W \approx 13.52$ for $N = 1000$ and $W \approx 27.04$ for $N = 2000$. The length of channel L is equal to 13.52 in both cases.

We maintain the nonequilibrium steady state by thermostatting the two species at different temperatures. To ensure that we can observe hydrodynamic behavior, we use a variant of the Lowe-Andersen (LA) thermostat [11], because it is local and momentum conserving. We modified the LA thermostat such that it regularly updates the relative kinetic energy of HH or CC pairs, sampling from Maxwell-Boltzmann distributions at temperatures T_H and T_C, respectively. In the simulations, we determine the temperature from the kinetic energy of the particles. T denotes the measured average temperature of the entire system, and $\Delta T/T$ is the relative temperature difference between the two species. We performed simulations at two different strengths of the thermal driving: in the weakly driven state, we applied the Lowe-Andersen thermostat to one particle pair per time step ($N = 1000$), in the strongly driven state the thermostat is applied to twenty particle pairs per time step ($N = 2000$). In order to be able to compare simulations on different system sizes, we define Γ_t, the rate of thermostatting, as the number of thermalizing collisions per time step divided by N. Thus, the weak and strong thermal driving in our simulation correspond to $\Gamma_t = 10^{-3}$ and $\Gamma_t = 10^{-2}$, respectively. All data for $\Delta T/T > 0.15$ were obtained with $\Gamma_t = 10^{-2}$. We find that the strength of the thermostat does influence the viscosity of the system (see Fig. S6 in SM [9]), but not our findings about the validity of the Onsager relations.

The sustained application of the double thermostat maintains a steady energy flow from the H to the C particles, ensuring that the two species have different average temperatures. Note that a steady energy flow imposes an "arrow of time" and therefore violates microscopic reversibility.

When a particle of either species encounters one of the flat hard walls of the channel, its velocity will either be reversed ("bounce back": B), or only its normal velocity will change sign ("specular": S). For a one-component fluid, the S and B collision rules roughly mimic slip and no-slip boundary condition (see, e.g., Ref. [12]). In real systems, the friction with the walls is determined by intermolecular interactions, but then the two species would have different adsorption profiles, even in equilibrium. The advantage of controlling the wall friction by kinematics, rather than by varying the particle-wall potential is that the different kinematic rules do not affect the density profiles at the walls, at least in equilibrium.

In our simulations, we studied the BB, BS, and SB cases, where the first and second letter refers to the cold and hot particles. We define the average velocity of the H and C particles as $v^{H,C} \equiv (1/N_{H,C}) \sum_{i=1}^{N_{H,C}} \mathbf{v}_i^{H,C}$. Then the fluxes J_H and J_C of the hot and cold particles are defined as $J_{H,C} = (N_{H,C}/L) \times v^{H,C}$, and the total flux $J_T = J_H + J_C$. We note that part of the flux of each species is due to advection of the bulk mixture by the fluid flow. For a given particle type, say for cold particles, the advection flux is given by $J_C^{\mathrm{adv}} = J_T \rho_C^{(B)}/(\rho_C^{(B)} + \rho_H^{(B)})$, where $\rho_{C,H}^{(B)}$ are the densities of the cold and hot particles in the bulk. The diffusive flux is then the remaining part of the particle flux: $J_D = J_C - J_C^{\mathrm{adv}}$.

In this model, we can study two kinds of cross-coupling between fluxes. First of all, in the bulk of the fluid, a force on one species will also induce a bulk flux in the other species. This cross-coupling is large, and hence testing the Onsager relations is easy. More interestingly, we can consider the whole system, including the boundary layers, and test how the presence of the walls creates a coupling between the total particle flux and the diffusive flux. This is particularly interesting in the BB case, for which there is no coupling unless the two species are at different temperatures. In the absence of surface effects, the eigenvectors of transport matrix [Eq. (1)] correspond to pure flow and pure diffusion. However, in the presence of walls, the transport matrix could develop off-diagonal elements mixing diffusion and flow.

We first determine the transport matrix for the bulk of the system and check whether this matrix satisfies the Onsager symmetry. Next, we determine the transformation that diagonalizes the bulk transport matrix. This transformation will only diagonalize the transport matrix of the whole system if there is no surface-induced coupling between diffusion and flow. Finally, we test if the transport matrix of
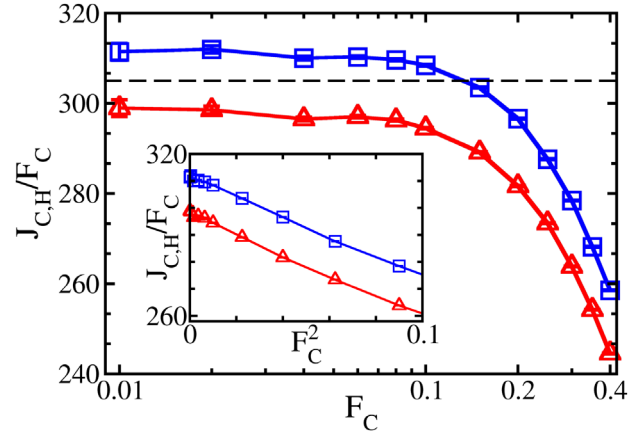

FIG. 2. Relation between the fluxes and the force F_C acting on cold particles only ($F_H = 0$) for the system with BB boundary conditions and $\Delta T/T = 0$. We plot the ratio J/F_C in order to visualize the range of validity of the linear response. The symbols represent the "cold" particles J_C/F_C (blue squares) and "hot" particles J_H/F_C (red triangles). In the inset, J/F_C is plotted against F_C^2 to quantify the lowest-order nonlinear term. All simulations in the main text were carried out with forces of magnitude 0.01, which is clearly deep within the validity of the linear response. A systematic overview of this relation for all parameters, can be found in SM (Figs. S2–S5) [9].

the whole system satisfies the Onsager symmetry, even for a thermally driven system.

We carry out all simulations in the linear regime (see Fig. 2); therefore, we can use any linearly independent pair of forces to determine the transport matrix. Once the matrix has been computed for a given set of forces, it can be transformed to any other set. Denoting the color forces on the hot and the cold particles by F_H and F_C, we performed one simulation with $\{F_H, 0\}$ and one with $\{0, F_C\}$. The color forces act along the x direction (see Fig. 1). To compute the transport matrix for the bulk of the fluid ($\mathcal{L}_{\alpha\beta}^{(B)}$), we study the relation between forces and fluxes along the length of the channel, in a slab of fluid of width 6σ for $\Gamma_t = 10^{-3}$ (8σ for $\Gamma_t = 10^{-2}$) that is sufficiently far removed from both walls to eliminate direct surface induced effects (the density profiles of the H and C particles are shown in Fig. S1 of Supplemental Material [9]).

Note that to compute the transport matrix of the bulk material, we only impose forces within the "bulk" slab, and only measure the fluxes in this slab. We impose infinitely thin specular walls between the fluid inside and outside the slab, to ensure that the color forces always act on the same set of particles. To correct for the fact that the specular walls suppress compositional fluctuations in the slab, we averaged the results over 800 simulations with independent initial conditions. In contrast, when computing the transport matrix of the whole system, we impose uniform forces along the channel throughout the system and measure the total resulting fluxes.
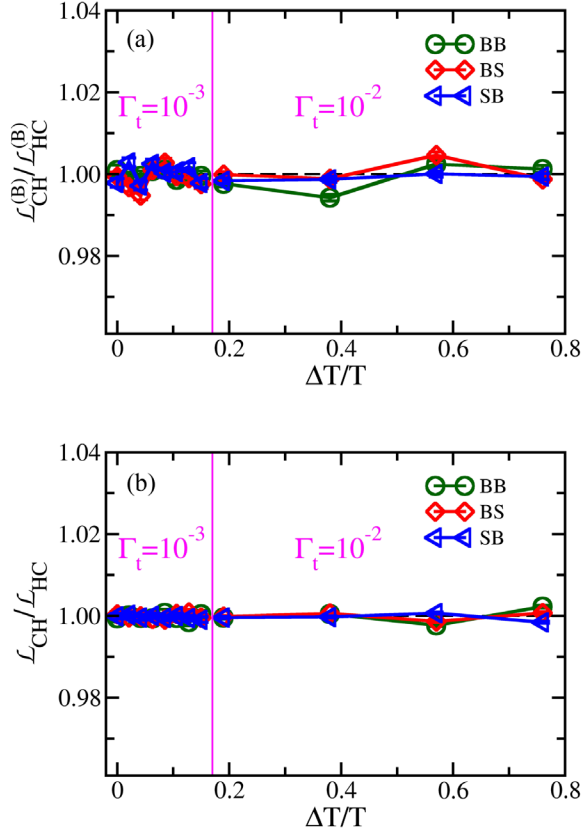
FIG. 3. Ratio of the off-diagonal elements of the transport matrix relating the flux of cold (C) and hot (H) particles subject to color forces F_C and F_H. The figure shows the results for weak ($\Gamma_t = 10^{-3}$) and strong thermal driving ($\Gamma_t = 10^{-2}$). (a) Results for the case where the applied forces and measured fluxes are confined to the bulk of the system. (b) Results for simulations in the entire channel (without the additional specular walls) with surfaces-induced coupling between diffusion and flow. Note that the SB and BS cases are distinct: one is obtained from the other by permuting S and B, and replacing ΔT with $-\Delta T$. In contrast, the BB case is even in ΔT. In spite of the linear dependence of the SB and BS transport coefficients on ΔT, the Onsager relations still seem to be satisfied. The error bars (about the size of the symbols) correspond to one standard deviation.

We carried out some 800 independent simulations for every data point. The length of a typical simulation was 6×10^6 time steps, where the length of each time step was $dt = 0.001$ in reduced units. Every run was preceded by an equilibration run of 10^6 time steps. Fluxes were measured every 6000 time steps. We verified that successive samples were not significantly correlated.

We first verified that the relation between forces and fluxes was linear for the conditions where we compute the transport matrices (see Fig. 2 and Figs. S2–S5 in SM [9]). In the linear regime, the relation between forces and fluxes can be described by Eq. (1). Note that in the bulk, the flux of the species on which the force acts is only slightly larger than the resulting flux of the other species. Such behavior is

to be expected as the force on one species causes a net flow of the mixture containing both species. In systems driven from the equilibrium state, the two species in the system (H and C) are at the same temperature, and we expect the Onsager relation to hold: $\mathcal{L}_{HC} = \mathcal{L}_{CH}$. However, in our thermally driven simulations of systems perturbed from a nonequilibrium steady state, we consider ΔT values that are up to 80% of the average temperature. Therefore, while we work in the regime where the driving forces are small, our simulations are very far out of equilibrium.

In what follows, we report both the transport matrix $\mathcal{L}^{(B)}$ for bulk of the system, and the transport matrix $\mathcal{L}$ for the whole system. As can be seen from Fig. 3(a) the transport matrices describing the relation between the color forces $F_H^{(B)}$ and $F_C^{(B)}$, and the particle fluxes $J_H^{(B)}$ and $J_C^{(B)}$ do satisfy the Onsager relations as expected for $\Delta T = 0$, but also for $\Delta T \neq 0$.

It is instructive to consider the eigenvectors of the matrix $\mathcal{L}^{(B)}$. In the absence of surface effects, the two (orthogonal) eigenvectors of this matrix correspond to forces that induce either bulk flow or diffusion. In the SM [9], we show the components of the matrix P that diagonalize $\mathcal{L}^{(B)}$. At equilibrium, P can be directly calculated from the composition of the bulk fluid. In the case where all particles move with the same average speed $v^{(B)}$, i.e., in the absence of diffusive fluxes, we would expect that $v^{(B)} = J_C^{(B)}/\rho_C^{(B)} = J_H^{(B)}/\rho_H^{(B)}$, where $\rho^{(B)}$ denotes the bulk density of either species. In other words, we expect diffusionless flow corresponding to $\rho_C^{(B)} J_H^{(B)} = \rho_H^{(B)} J_C^{(B)}$. As we know the bulk densities of our system (see SM [9]), we can predict the matrix that diagonalizes $\mathcal{L}^{(B)}$ and compare it with numerical result. The data in the SM [9] confirm that the situation corresponding to pure diffusion and pure flow are indeed eigenvectors of $\mathcal{L}^{(B)}$.

Figure 3(b) shows the ratio of off-diagonal elements of $\mathcal{L}$ obtained from simulations in the entire channel. To quantify the coupling between diffusion and flow due to the boundaries of the channel, we apply the transformation that diagonalizes $\mathcal{L}^{(B)}$, to $\mathcal{L}$ of the entire system. The transformed matrix $\mathcal{L}'$ would be diagonal in the absence of the diffusion-flow coupling. The results for the (normalized) off-diagonal elements of $\mathcal{L}'$ are shown in Fig. 4.

We note that for the BB boundary condition, the off-diagonal element coupling diffusive flux (D) and total flow (T) vanishes at $\Delta T = 0$, as it should, because the boundaries have the same effect on both species. In contrast, for the BS and SB cases, there is diffusio-capillary coupling even at $\Delta T = 0$. More importantly: the numerical data are all compatible with the assumption that the Onsager relations still hold, even for diffusio-capillary coupling in a driven system. We stress that the thermal driving can be very strong: up to $\Delta T/T = 0.8$. The Onsager symmetries are also satisfied in the BB case, where there is no coupling at
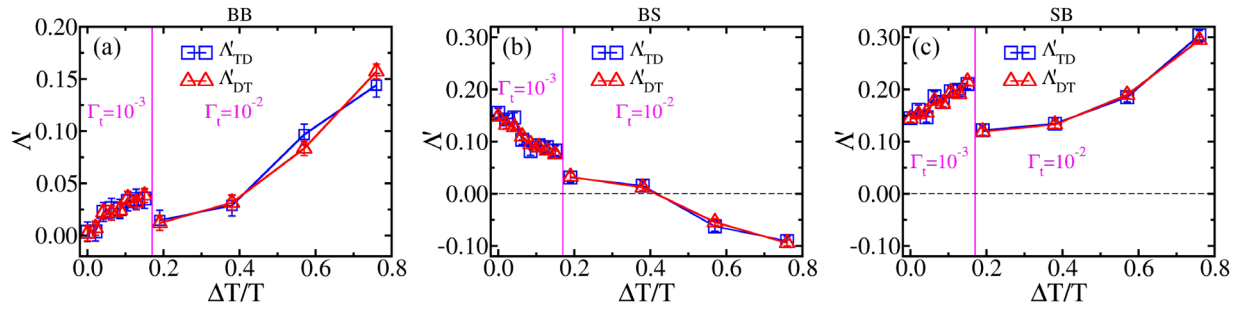
FIG. 4. Ratio of the off-diagonal elements of the transport matrix, describing the coupling between diffusion and flow for three versions of the boundary conditions: *BB* (a), *BS* (b), and *SB* (c). The figure shows the normalized off-diagonal transport coefficients for weak ($\Gamma_t = 10^{-3}$) and strong thermal driving ($\Gamma_t = 10^{-2}$). We have plotted the normalized matrix elements $\Lambda'_{TD} \equiv \mathcal{L}'_{TD} / \sqrt{\mathcal{L}'_{TT}\mathcal{L}'_{DD}}$ (blue) and $\Lambda'_{DT} \equiv \mathcal{L}'_{DT} / \sqrt{\mathcal{L}'_{TT}\mathcal{L}'_{DD}}$ (red). Note that the values of the elements of the transport matrix depend on the strength of the thermal driving. However, the coincidence of red and blue lines shows that Onsager symmetry seems to be conserved. The unnormalized matrix $\mathcal{L}'$ is given in SM [9].

$\Delta T = 0$ and the cross coupling is completely due to the thermal driving.

Our results strongly suggest that the Onsager relations are robust outside the range of conditions for which they were derived. Of course, absence of evidence is not evidence for absence, and hence there certainly could be driven or active systems, e.g., field-aligned polar or chiral active "swimmers," which violate time-reversal symmetry, for which the Onsager relations are more likely to fail. It would be important to understand if and when the Onsager relations fail.

*Also at Yusuf Hamied Department of Chemistry, University of Cambridge, Cambridge, United Kingdom.
†jd489@cam.ac.uk
‡df246@cam.ac.uk

[1] L. Onsager, Phys. Rev. **37**, 405 (1931).
[2] S. Kjelstrup and D. Bedeaux, *Non-Equilibrium Thermodynamics of Heterogeneous Systems* (World Scientific, Singapore, 2020).
[3] A. E. Allahverdyan and T. M. Nieuwenhuizen, Phys. Rev. E **62**, 845 (2000).
[4] D. Miller, Chem. Rev. **60**, 15 (1960).
[5] J. Xu, S. Kjelstrup, D. Bedeaux, A. Rosjorde, and L. Rekvig, J. Colloid Interface Sci. **299**, 452 (2006).
[6] G. Arya, H. C. Chang, and E. J. Maginn, J. Chem. Phys. **115**, 8112 (2001).
[7] H. Yoshida, S. Marbach, and L. Bocquet, J. Chem. Phys. **146**, 194702 (2017).
[8] S. Ramirez-Hinestrosa and D. Frenkel, Eur. Phys. J. B **94**, 199 (2021).
[9] See Supplemental Material at http://link.aps.org/supplemental/10.1103/PhysRevLett.129.238002 for additional technical details on performed simulations, supplementary data on density profiles, force-flux relations, effects of the thermostat on fluid viscosity, and full details on the computed matrices.
[10] J. D. Weeks, D. Chandler, and H. C. Andersen, J. Chem. Phys. **54**, 5237 (1971).
[11] C. P. Lowe, Europhys. Lett. **47**, 145 (1999).
[12] G. Gompper, T. Ihle, D. M. Kroll, and R. G. Winkler, in *Advanced Computer Simulation Approaches for Soft Matter Sciences III*, Advances in Polymer Science Vol. 221, edited by C. Holm and K. Kremer (Springer, New York, 2009), pp. 1–87.